

Thermochemistry of Nitrogen Doped Reduced Graphene Oxides

Stefania Sandoval[‡], Elayaraja Muthuswamy[†], Jiewei Chen[†], Amparo Fuertes[‡], Gerard Tobias[‡],
Alexandra Navrotsky^{†*}

[†]Peter A. Rock Thermochemistry Laboratory and NEAT ORU, University of California Davis,
Davis, CA 95616, USA

[‡]Institut de Ciència de Materials de Barcelona (ICMAB-CSIC), Campus de la UAB, 08193
Bellaterra, Spain

*Corresponding author.

E-mail address: anavrotsky@ucdavis.edu (A.Navrotsky).

Abstract

The thermodynamic stability of a series of nitrogen - doped reduced graphene oxides prepared by ammonolysis of graphene oxide has been investigated by high temperature oxidation calorimetry. In terms of enthalpy and depending on the concentration of nitrogen, the nitrogen-doped reduced graphene oxides can be up to $73 \text{ kJ}\cdot\text{mol}^{-1}$ more stable than graphite plus nitrogen. There is a linear relationship between the nitrogen content and the formation enthalpy, which indicates a decrease in stability with increasing nitrogen content.

Keywords: N-doped graphene oxide, calorimetry, stability

1. Introduction

Among the various nanoscale allotropes of carbon, graphene has captured the imagination of scientists worldwide since their report in 2004 by Geim and coworkers[1]. The enormous interest in graphene stems from its unique and extraordinary physical and chemical properties including large surface area[2], high thermal and electrical conductivity[3], mechanical strength, transparency and structural flexibility[4]. The versatility of the material, whose structure is readily modified by a variety of approaches, has paved the way toward the preparation of derivatives with improved performance that can potentially translate into next generation applications in wide ranging fields such as energy conversion and storage[5, 6], catalysis[7, 8] electronics[2, 9] and composite materials [10, 11]. Embedding graphene within ceramic matrices is a promising approach for the large scale production of materials with enhanced mechanical properties[12]. For instance, Simsek *et al.* reported improvements in the electrical conductivity and fast heat release of aluminum nitride, a dielectric material with potential applications such as microelectromechanical systems (MEMs) or light emitting diodes (LEDs), after using graphene nanoplatelets as filler[13]. In a more recent study, the author took advantage of the properties of both the filler and the ceramic structure to obtain YSZ-graphene composites with mixed-ionic and electronic conduction and enhanced stability [14].

Graphene oxide (GO) is a chemically functionalized variant of graphene containing oxygen in the form of hydroxyl and epoxide groups in the defect free regions and carboxyl, carbonyl, and phenol groups on the sheet edges[15]. It is typically prepared by oxidation of graphite into graphitic oxide and subsequent exfoliation of the layered structure[15]. Due to difficulties in the large scale production and processing of single layer graphene, its oxidized form is considered a promising alternative. The functional groups on the surface of GO makes it

water dispersible[16]and attractive for catalytic[17]and biomedical applications[18]. GO properties can be modified by controlling morphology and size[19]. In addition,the reactivefunctional groups on the GO surface can be employed for the covalent attachment of selected (bio)molecules [20]and inorganic nanoparticles[21]or for chemical doping[22]. Chemical doping is an effective method to tune electronic, magnetic and thermal properties, thus broadening the range of applications[23, 24].

Substitutional replacement by heteroatoms such as nitrogen and boron is a popular chemical doping method for GO[25, 26].Nitrogen doping has attracted special interest due to the potential application of the resulting materials in a variety of fields including electrocatalysis[27, 28], energy storage and harvesting[29-31], and flame retardant additives[32-35].A wide range of methods have been developed to achieve varying nitrogen concentrations[36-38].The high temperature reaction of GO with NH_3 gas can achieve doping levels as high as 13 wt. %[39-41].The oxygen content in GO and the reaction temperature playkey roles in the final nitrogen content.The presence of oxygen facilitates functionalization by other chemical groups, thus favoring the formation of C-N bonds[42].Different bonding environments for nitrogen have been identified in the graphene structure, the most commonly reported beingpyridinic, pyrrolicand graphitic groups[36].Their relative abundance is determinedby the synthetic method and the reaction parameters.GO processed under such reducing conditions has lower oxygen content and is called reduced graphene oxide (rGO)[43]. The reduction of oxygen content in rGO partially restores graphene-like properties[44].The electronic and structural changes caused by doping confer new interesting attributes[44].N-containing groupsallow tuning the band gap of the conjugated lattice[45] andenhance the thermal oxidation stability of reduced graphene oxide in air[39].

GO was first synthesized in 1859[46] and, despite extensive development of synthetic methods and study of properties in subsequent decades, the thermochemistry and stability of GO and its derivatives relative to other forms of carbon are relatively unexplored. We have successfully investigated the thermodynamic stability of nanodiamonds[47] and carbon onions using high temperature direct oxidation calorimetry [48]. Suslova *et al.* have determined the formation and combustion enthalpy of several N-containing carbon allotropes by bomb calorimetry[49]. In the present work, we have carried out high temperature oxidation calorimetry of a series of nitrogen doped rGO samples with varying contents of nitrogen (7.1 to 11.4 at. %) and report their formation enthalpies at room temperature. We conclude that, although nitrogen stabilizes the rGO phase energetically, such stabilization decreases with increasing nitrogen doping.

2. Materials and Methods

2.1. Synthesis of graphene oxide

Graphene oxide was prepared via a modified Hummer's method[41]. Briefly, 5 g of graphite powder (< 20 μm , Sigma-Aldrich) were treated with a mixture of concentrated H_2SO_4 (115 mL) and NaNO_3 (2.5 g). This reaction mixture was cooled to 0 $^\circ\text{C}$ and left for 30 min. Next, KMnO_4 (15 g) was added slowly. After stirring for 30 min at about 35 $^\circ\text{C}$, distilled water (230 mL) was slowly added maintaining the reaction temperature at 98 $^\circ\text{C}$ for 2 h. Finally, additional water (1 L) and 30% H_2O_2 (5 mL) were added and the reaction mixture was cooled down. The resulting material was purified by subsequent centrifugation and washing with distilled water until the pH of the solution was neutral.

2.2. Preparation of nitrogen doped reduced graphene oxide (*N-doped rGO*)

N-doped rGO was prepared following a previously reported protocol[41]. 100 mg of graphene oxide were spread in an alumina boat. The alumina boat containing the GO was then placed in the center of a silica tube inside a horizontal furnace. The whole system was purged under nitrogen for 1 h to remove air from the system before introducing ammonia gas (Carburos Metálicos 99.99%) at a flow rate of 300 mL·min⁻¹. Samples were heated for 1 h at temperatures between 500 and 800 °C, to obtain simultaneous reduction and doping of graphene oxide.

2.3. Morphology of *N-doped rGO* samples

The morphology of *N-doped rGO* samples was determined by means of microscopic analyses. TEM and SAED patterns were obtained using a JEOL 1210 microscope, operating at 120 kV. HRTEM images were acquired using a FEI, Tecnai microscope operating at 200 kV. Samples were prepared by dispersing a small amount of powder in hexane using bath sonication. Afterwards, the dispersions were placed dropwise onto a lacey carbon support grid.

2.4. Elemental composition of the samples

Elemental analyses (EA) were performed on a Thermo Scientific™ FLASH 2000 Series CHNS Analyzer using a Mettler Toledo MX5 microbalance. The atomic composition of the samples (C, N, O) and the distribution of oxygen and nitrogen in different bonding environments were obtained by X-ray photoelectron spectroscopy (XPS), using a Kratos AXIS ultra DLD spectrometer with Al K α radiation. All samples were introduced in the preparation chamber as received and placed on a copper substrate for analysis. A general survey scan performed on the samples confirmed the presence of C, N, and O as the only constituent elements. High resolution

spectra over the C 1s, O 1s and N 1s regions were registered and employed to determine the elemental composition of each of the samples.

2.5. High temperature oxidation calorimetry

The oxidation enthalpy of the samples was determined by high temperature oxidation calorimetry using an AlexSYSSetaramisoperibol Tian-Calvet twin microcalorimeter. Approximately 1 mg pellets were made using a pellet press, weighed on a microbalance and dropped from room temperature (25 °C) into a silica glass crucible containing a small piece of silica wool at its bottom in the calorimeter maintained at 800 °C. The samples were rapidly oxidized to CO₂ gas at the calorimeter temperature by the reaction: C(s, 25 °C) + O₂(g, 800 °C) → CO₂(g, 800 °C). Air was flushed through the area close to the silica wool at 40 mL·min⁻¹ and through the calorimeter assembly at 50 mL·min⁻¹ to ensure complete oxidation of samples to CO₂. Oxygen atmosphere caused the samples to flare during the drop and so air atmosphere was chosen for these experiments to ensure that oxidation of the samples occurs only in the calorimeter chamber. Measurements were repeated 8-12 times to obtain statistically reliable enthalpy values. The calorimeter was calibrated against the heat content of platinum pieces. The procedure followed here is similar to that established previously in the work on nanodiamonds and onion-like carbons by Costa *et al.* [47, 48].

3. Results and discussion

Four samples were prepared following a previously reported methodology using GO and NH₃ gas at different temperatures (500 °C, 600 °C, 700 °C and 800 °C) [41]. In agreement with previous observations [41], electron microscopy analyses of the prepared samples reveal the presence of few-layered N-doped rGO. The wrinkled morphology of N-doped rGO is clearly visible in the TEM image of Figure 1a. The intensity profile along the diffraction spots of the

corresponding selected electron diffraction (SAED) pattern (Figure 1b) indicates the presence of a single layered specimen (the inner spots show about twice the intensity of the outer spots)[50]. The elongated appearance of the spots might arise from lack of crystallinity due to structural defects. A HRTEM image of the sample prepared at 500 °C is included in Figure 1c. The line profile across the edge of the flake indicates the presence of four layers with the expected separation of *ca.* 0.34 nm. Additional analyses are include in Figure S1 confirming that the prepared samples consists of few-layered N-doped rGO.

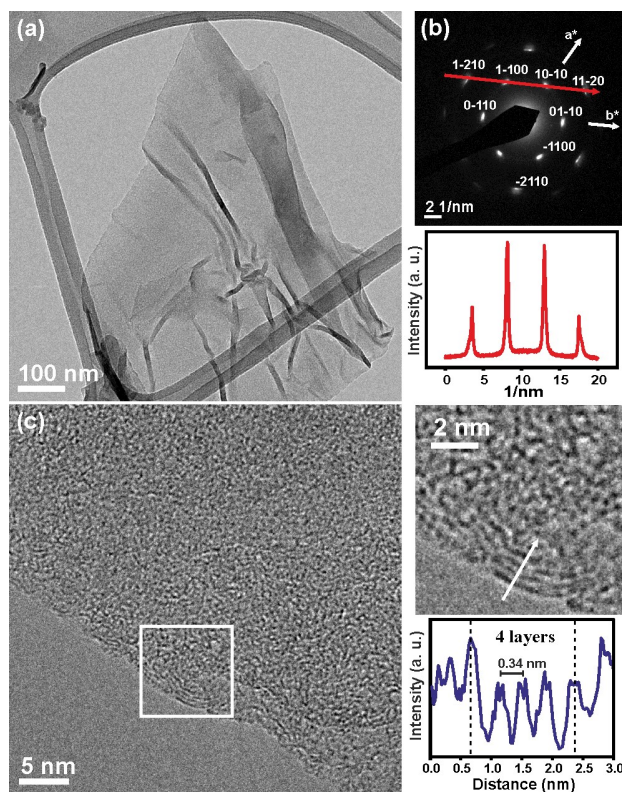


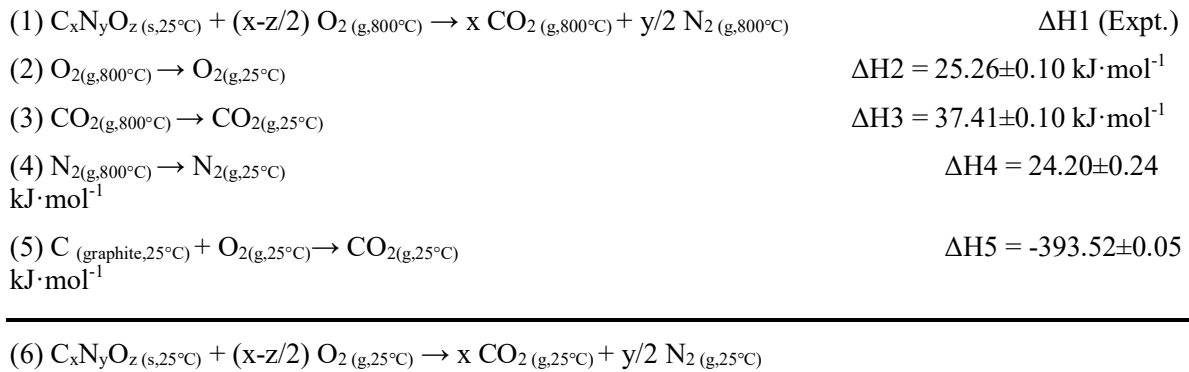
Figure 1. (a) Transmission electron microscopy image and (b) SAED pattern and diffracted intensity profile taken along the 1–210 to 11–20 axis for a sample of N-doped rGO prepared at 700 °C. (c) HRTEM of N-doped rGO prepared at 500 °C; an image magnification of the area marked with a white square is included on the right panel along with the intensity profile across the edge.

The reduced graphene oxide samples doped with varying amounts of nitrogen were analyzed by calorimetry. The measured (800 °C) and calculated (25 °C) oxidation enthalpies of the resulting N- doped rGO samples along with their formation enthalpies from elements (25 °C) are listed in Table 1. The table also includes oxidation and formation enthalpies calculated with respect to the carbon content of each sample(atomic composition, at. %), as determined by X-ray photoelectron spectroscopy (XPS). The calculations are based on the thermodynamic cycle in Table 2.XPS has been widely employed to determine the atomic composition of N-containing graphene derivatives.[40, 51-53] Nevertheless, in order to confirm the composition of the synthesized samples, elemental analysis (wt. %) was also performed (Table S1).

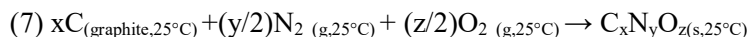
Table 1. Atomic composition, measured oxidation enthalpies and calculated room temperature oxidation and formation enthalpies of nitrogen-doped rGO samples.

Sample #	Atomic Composition			$\Delta H_{ox}, 800\text{ }^{\circ}\text{C}$ (kJ·mol ⁻¹)	$\Delta H_{ox}, 25\text{ }^{\circ}\text{C}$ (kJ·mol ⁻¹)	$\Delta H_{ox}, 25\text{ }^{\circ}\text{C}$ (kJ·g ⁻¹ ·C-atom ⁻¹)	$\Delta H_f, 25\text{ }^{\circ}\text{C}$ (kJ·mol ⁻¹)	$\Delta H_f, 25\text{ }^{\circ}\text{C}$ (kJ·g ⁻¹ ·C-atom ⁻¹)
	C	N	O					
1	90.6	7.1	2.3	-312.07±0.88	-324.42±1.07	-358.08±1.18	-38.40±0.93	-42.38±1.03
2	89.1	9.0	1.9	-314.33±2.25	-326.63±2.44	-366.59±2.74	-28.72±2.30	-32.23±2.58
3	87.5	10.4	2.1	-315.09±1.27	-327.27±1.46	-374.02±1.67	-17.85±1.31	-20.40±1.50
4	85.5	11.4	3.1	-310.38±2.18	-322.54±2.36	-377.24±2.76	-13.92±2.22	-16.28±2.60

Table 2. Thermodynamic cycle used to calculate the room temperature oxidation enthalpy and formation enthalpy for the nitrogen-doped rGO samples.



$$\Delta H_{(ox,25^{\circ}C)} = \Delta H1 + (x-z/2) \Delta H2 - \Delta H3 - (y/2) \Delta H4$$



$$\Delta H_{(f,25^{\circ}C)} = x \Delta H5 - \Delta H_{(ox,25^{\circ}C)}$$

While all N-doped rGO samples exhibit highly exothermic oxidation enthalpies (in the range of -327 to -322 kJ·mol⁻¹), these values are significantly lower in magnitude than the corresponding oxidation enthalpy for graphite (-393.5 kJ·mol⁻¹). For comparison, the oxidation enthalpies of major carbon allotropes are given in Table 3. Thus, N-doped rGO appears to be more stable in enthalpy than graphite by 65-73 kJ·mol⁻¹. Unlike graphite, purely formed by C atoms, N-doped rGO samples contain partially oxidized surfaces, as in the case of the carboxylic functionalized nanodiamonds, as well as nitrogen in their structure. Therefore, less heat is released on their complete combustion to CO₂ and N₂ (Table 2), compared to pure carbon allotropes. In fact, since the measured enthalpy refers to a material containing C, N, and O and not to pure carbon, strictly speaking, N-doped rGOs are not allotropes of carbon but different phases in a multicomponent system.

Table 3. Room temperature oxidation enthalpies and enthalpies relative to graphite (plus O₂ and N₂ as appropriate) of various carbon forms.

Allotrope		$\Delta H_{ox,800^{\circ}C} (kJ \cdot mol^{-1})$	$\Delta H_{ox,25^{\circ}C} (kJ \cdot mol^{-1})$	$\Delta H_{t,25^{\circ}C} (kJ \cdot mol^{-1})$
Graphite			-393.52±0.05	0.0
Diamond			-395.42±0.50	1.9±0.50
Fullerene, C ₆₀			-432.76±0.19	39.24±0.20
Nanodiamond(COOH)	4.5±0.4 nm	-329.25±0.67	-344.08±2.03	-49.44±2.03
	80.3±5.5 nm	-365.97±0.84	-379.45±1.82	-14.07±1.82
Carbon onion	UD90, 1800 °C	-396.04±0.67	-408.14±0.68	14.62±0.68
	UD50, 1300 °C	-382.67±0.78	-394.77±0.78	1.25±0.78
N-doped rGO	7.1% N	-312.07±0.88	-324.42±1.07	-69.10±1.07
	9.0% N	-314.33±2.25	-326.63±2.44	-66.89±2.44
	10.4% N	-315.09±1.27	-327.27±1.46	-66.25±1.46
	11.4% N	-310.38±2.18	-322.54±2.36	-70.98±2.36

To evaluate the effect of nitrogen on thermodynamic stability, care has been taken during the synthesis to ensure that the oxygen content (1.9-3.1 at. %) does not vary significantly between the four N-doped rGO samples. To identify trends in the relation between sample composition and heat effects, the calculated room temperature oxidation enthalpies in $\text{kJ}\cdot\text{mol}^{-1}$ and $\text{kJ}\cdot\text{g}^{-1}\cdot\text{C}\cdot\text{atom}^{-1}$ are plotted against the carbon content of the samples (Figure 2). While a clear trend cannot be established in the oxidation enthalpy ($\text{kJ}\cdot\text{mol}^{-1}$) vs. carbon content plot (Figure 2-(a)), the enthalpies calculated per gram atom of carbon ($\text{kJ}\cdot\text{g}^{-1}\cdot\text{C}\cdot\text{atom}^{-1}$) indicate more favorable thermodynamic stability with increasing carbon content (Figure 2(b)). The stability decreases linearly at first with decreasing carbon content and then evolves to a more gradual change, reaching the least stable value for the sample with 85.5 at. % C (11.4 at. % N). When the same data set is plotted against the nitrogen content of the samples (Figure 2), the plots reveal similar trends. Although the enthalpies in $\text{kJ}\cdot\text{mol}^{-1}$ again show scatter (Figure 2(a)), the sample prepared at 500 °C (11.4 at. % N) shows a higher energetic stability than the sample prepared at 800 °C (7.1 at. % N) in agreement with the report of Sandoval *et al.*[39]. When the data are represented in $\text{kJ}\cdot\text{g}^{-1}\cdot\text{C}\cdot\text{atom}^{-1}$ a clear trend is observed (Figure 2(b)).

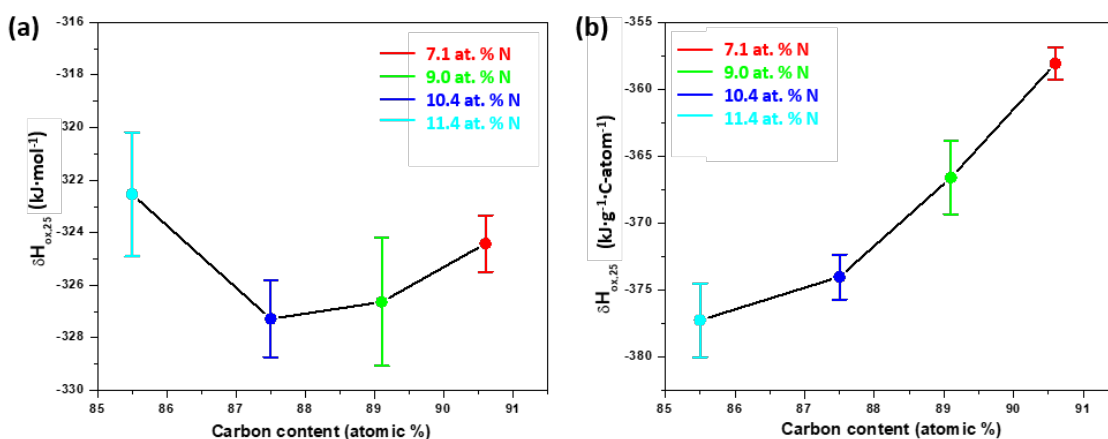


Figure 2. Room temperature oxidation enthalpies of N-rGO samples in (a) $\text{kJ}\cdot\text{mol}^{-1}$ and in (b) $\text{kJ}\cdot\text{g}^{-1}\cdot\text{C}\cdot\text{atom}^{-1}$ plotted against carbon content (atomic percent).

A linear relationship is seen between the nitrogen content and calculated enthalpies of oxidation, which become more exothermic with increasing nitrogen content, indicating diminishing energetic stability, as it can be observed in **Figure 3 (b)**.

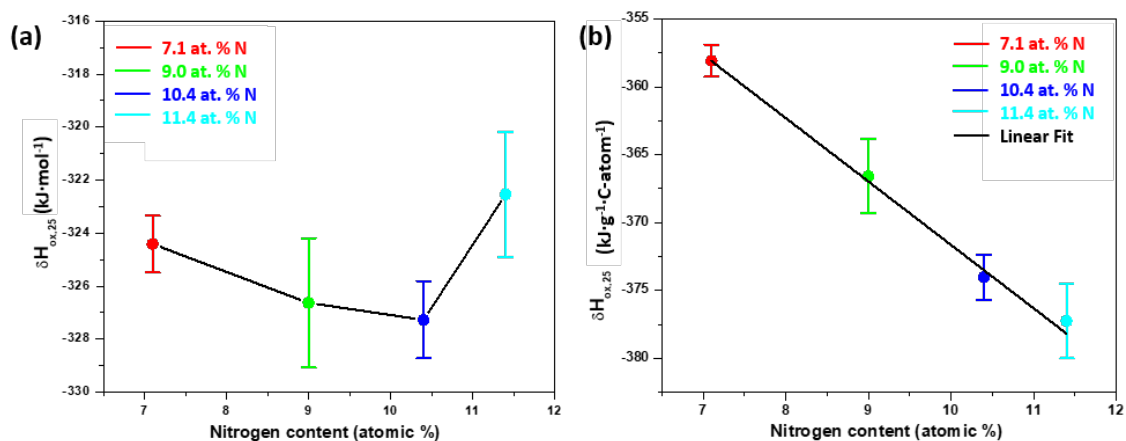


Figure 3. Room temperature oxidation enthalpies of N-rGO samples in (a) $\text{kJ}\cdot\text{mol}^{-1}$ and in (b) $\text{kJ}\cdot\text{g}^{-1}\cdot\text{C}\cdot\text{atom}^{-1}$ plotted against atomic percent of nitrogen.

The formation enthalpies of these samples were calculated using equation 7 and are given in Table 1. They are exothermic ranging between -12 and -39 $\text{kJ}\cdot\text{mol}^{-1}$ and become more negative with increasing carbon content. The values become slightly more exothermic when calculated with respect to gram atom carbon (Figure 4). Both plots reveal similar trends confirming more favorable energetic stability with increasing carbon content.

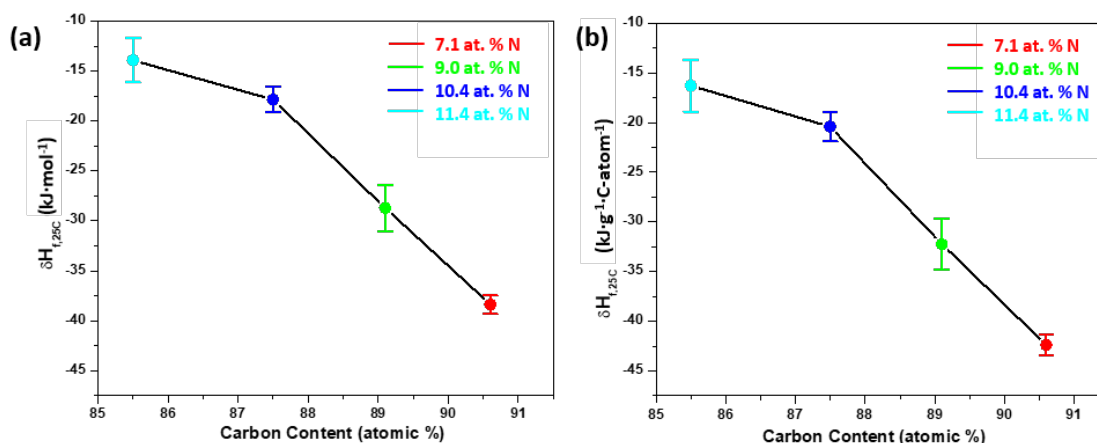


Figure 4. Formation enthalpies of N-rGO samples plotted against atomic percent of carbon in (a) $\text{kJ}\cdot\text{mol}^{-1}$ and (b) $\text{kJ}\cdot\text{g}^{-1}\cdot\text{C}\cdot\text{atom}^{-1}$.

The formation enthalpies show a linear trend with nitrogen content (Figure 5), showing that the substitution of nitrogen is energetically destabilizing. This study clearly indicates that formation of a nitrogen-free sample with oxygen is more thermodynamically favorable than nitrogen incorporation.

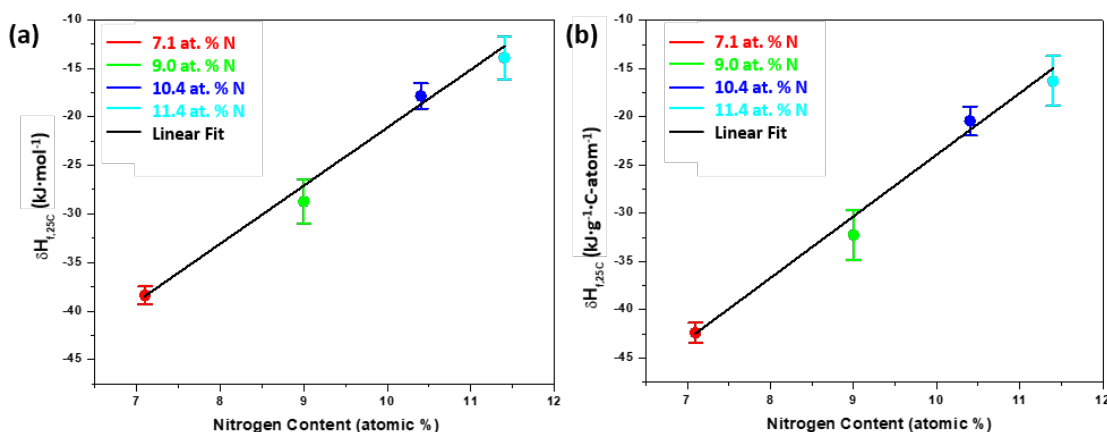


Figure 5. Formation enthalpies of N-rGO samples plotted against atomic percent of nitrogen in (a) $\text{kJ}\cdot\text{mol}^{-1}$ and (b) $\text{kJ}\cdot\text{g}^{-1}\cdot\text{C}\cdot\text{atom}^{-1}$.

Sandoval *et al.* considered a simplified model of a graphene fragment and its variants containing each type of nitrogen (pyrrolic, pyridinic and graphitic N) and calculated the

combustion enthalpies of the fragments using mean bond enthalpies [39]. The calculated Gibbs energy (ΔG) associated with each of those reactions showed that the reaction of the undoped fragment would be more spontaneous. The calculations were performed for 500 °C since this was the average onset combustion temperature of the analyzed samples as determined by thermogravimetric analysis. They suggested that variations in thermal stability (onset of oxidation reactions) were related to their calculated trends in thermodynamic stability. Because thermal stability reflects both thermodynamic and kinetic factors we consider these arguments to qualitatively support energetic stabilization by nitrogen substitution.

Table 4. N, C and O content in N-rGO samples determined by X-ray photoelectron spectroscopy

Sample	Nitrogen (at. %)			Oxygen (at. %)			Carbon (at. %)
	PyridinicN	PyrrolicN	GraphiticN	O=C-O	O=C	O-C	
	4.8	4.2	2.4	1.1	0.9	1.1	
11.4 % N	11.4			3.1			85.5
	4.1	3.7	2.6	0.7	0.7	0.7	
10.4 % N	10.4			2.1			87.50
	3.2	3.2	2.6	0.5	0.6	0.8	
9.0 % N	9.0			1.9			89.1
	2.8	2.3	2.0	0.6	0.8	0.9	
7.1 % N	7.1			2.3			90.6

A wide range of methods have been published for doping nitrogen into graphene and related structures. The distribution of nitrogen environments in the structure has been observed to vary with different preparation methods[36]. In this work, rGO samples have been prepared by post treatment of graphene oxides with ammonia at high temperatures (500-800 °C). This method typically results in samples rich in pyridinic and pyrrolic nitrogen due to the ease of incorporation of nitrogen at the edges. A higher annealing temperature is required to promote the formation of graphitic nitrogen (for high resolution N1s and O1s XPS spectra see Figure S2 and Figure S3, respectively)[36]. In the samples investigated here, the distribution of the nitrogen

atoms in the three different bonding configurations does not vary significantly at different nitrogen concentrations (Table 4). Therefore, it is not possible to deconvolute the effect of different nitrogen centers on the resulting trends in thermodynamic properties.

4. Conclusions

We have experimentally determined the oxidation enthalpies of a series of N-doped rGO samples with N contents ranged between 7.1 and 11.7 at. % by high temperature (800°C) oxidation calorimetry studies. Our results confirm that the nitrogen doped reduced graphene oxide samples are significantly more stable in enthalpy than pure graphite and diamond. This reflects the incorporation of both oxygen and nitrogen and their resulting multicomponent nature. Formation enthalpies ($\Delta H_{f,25^\circ\text{C}}$) indicate more favorable energetics of materials with higher carbon contents. As a consequence, the formation of a nitrogen-free sample (or one with low N content) is more favored thermodynamically. A linear decrease in the energetic stability with increasing nitrogen content is observed within the studied range. Thus oxygen stabilizes the rGO phases while nitrogen destabilizes them. Thus, thermodynamic stabilization by nitrogen doping is not seen and therefore cannot be responsible for the enhanced thermal stability previously reported in N-doped rGO samples, and kinetic factors must be considered. The present study contributes toward understanding the properties of emerging heteroatom-enriched graphene derivatives.

Acknowledgments

The calorimetric studies at UC Davis were supported by the Fluid Interface Reactions, Structures and Transport (FIRST) Center, an Energy Frontier Research Center funded by the U.S. Department of Energy, Office of Science and Office of Basic Energy Sciences. We acknowledge financial support from the Spanish Ministry of Economy and Competitiveness

through MAT2017-86616-R grant and the “Severo Ochoa” Programme for Centres of Excellence in R&D (SEV-2015-0496). We thank Gustavo Costa for helpful suggestions concerning the measurements. The XPS data were acquired at the Laboratorio de Microscopías Avanzadas (LMA) - Instituto de Nanociencia de Aragón (INA).

Appendix A. Supplementary data

References

- [1] K.S. Novoselov, A.K. Geim, S.V. Morozov, D. Jiang, Y. Zhang, S.V. Dubonos, I.V. Grigorieva, A.A. Firsov, Electric Field Effect in Atomically Thin Carbon Films, *Science* 306 (2004) 666-669.
- [2] M.D. Stoller, S. Park, Y. Zhu, J. An, R.S. Ruoff, Graphene-Based Ultracapacitors, *Nano Lett.* 8 (2008) 3498-3502.
- [3] A.A. Balandin, S. Ghosh, W. Bao, I. Calizo, D. Teweldebrhan, F. Miao, C.N. Lau, Superior Thermal Conductivity of Single-Layer Graphene, *Nano Lett.* 8 (2008) 902-907.
- [4] R.S. Edwards, K.S. Coleman, Graphene synthesis: relationship to applications, *Nanoscale* 5 (2013) 38-51.
- [5] L. Dai, Functionalization of Graphene for Efficient Energy Conversion and Storage, *Acc. Chem. Res.* 46 (2013) 31-42.
- [6] J. Mao, J. Iocozzia, J. Huang, K. Meng, Y. Lai, Z. Lin, Graphene aerogels for efficient energy storage and conversion, *Energ. Environ. Sci.* 11 (2018) 772-799.
- [7] B.F. Machado, P. Serp, Graphene-based materials for catalysis, *Catal. Sci. Technol.* 2 (2012) 54-75.
- [8] S.M. Tan, M. Pumera, Two-Dimensional Materials on the Rocks: Positive and Negative Role of Dopants and Impurities in Electrochemistry, *ACS Nano* 13 (2019) 2681-2728.
- [9] B. Wang, W. Huang, L. Chi, M. Al-Hashimi, T.J. Marks, A. Facchetti, High-k Gate Dielectrics for Emerging Flexible and Stretchable Electronics, *Chem. Rev.* 118 (2018) 5690-5754.
- [10] Z. Chen, Z. Li, J. Li, C. Liu, C. Lao, Y. Fu, C. Liu, Y. Li, P. Wang, Y. He, 3D printing of ceramics: A review, *J. Eur. Ceram. Soc.* 39 (2019) 661-687.
- [11] V.S. Kudyakova, R.A. Shishkin, A.A. Elagin, M.V. Baranov, A.R. Beketov, Aluminium nitride cubic modifications synthesis methods and its features. Review, *J. Eur. Ceram. Soc.* 37 (2017) 1143-1156.
- [12] F.d. Río, M.G. Boado, A. Rama, F. Guitián, A comparative study on different aqueous-phase graphite exfoliation methods for few-layer graphene production and its application in alumina matrix composites, *J. Eur. Ceram. Soc.* 37 (2017) 3681-3693.

- [13] I.N.G. Simsek, A. Nistal, E. García, D. Pérez-Coll, P. Miranzo, M.I. Osendi, The effect of graphene nanoplatelets on the thermal and electrical properties of aluminum nitride ceramics, *J. Eur. Ceram. Soc.* 37 (2017) 3721-3729.
- [14] D. Marinha, M. Belmonte, Mixed-ionic and electronic conduction and stability of YSZ-graphene composites, *J. Eur. Ceram. Soc.* 39 (2019) 389-395.
- [15] K. Krishnamoorthy, M. Veerapandian, K. Yun, S.J. Kim, The chemical and structural analysis of graphene oxide with different degrees of oxidation, *Carbon* 53 (2013) 38-49.
- [16] J. Luo, L.J. Cote, V.C. Tung, A.T.L. Tan, P.E. Goins, J. Wu, J. Huang, Graphene Oxide Nanocolloids, *J. Am. Chem. Soc.* 132 (2010) 17667-17669.
- [17] T.-F. Yeh, C.-Y. Teng, S.-J. Chen, H. Teng, Nitrogen-Doped Graphene Oxide Quantum Dots as Photocatalysts for Overall Water-Splitting under Visible Light Illumination, *Adv. Mater.* 26 (2014) 3297-3303.
- [18] Z. Liu, J.T. Robinson, X. Sun, H. Dai, PEGylated Nanographene Oxide for Delivery of Water-Insoluble Cancer Drugs, *J. Am. Chem. Soc.* 130 (2008) 10876-10877.
- [19] J. Kim, L.J. Cote, F. Kim, W. Yuan, K.R. Shull, J. Huang, Graphene Oxide Sheets at Interfaces, *J. Am. Chem. Soc.* 132 (2010) 8180-8186.
- [20] I.N.G. Simsek, A. Nistal, E. García, D. Pérez-Coll, P. Miranzo, M.I. Osendi, The effect of graphene nanoplatelets on the thermal and electrical properties of aluminum nitride ceramics, *Journal of the European Ceramic Society* 37 (2017) 3721-3729.
- [21] D. Marinha, M. Belmonte, Mixed-ionic and electronic conduction and stability of YSZ-graphene composites, *Journal of the European Ceramic Society* 39 (2019) 389-395.
- [22] M. Kaur, M. Kaur, V.K. Sharma, Nitrogen-doped graphene and graphene quantum dots: A review on synthesis and applications in energy, sensors and environment, *Adv. Colloid. Interface Sci.* 259 (2018) 44-64.
- [23] Y. Li, Y. Zhao, H. Cheng, Y. Hu, G. Shi, L. Dai, L. Qu, Nitrogen-Doped Graphene Quantum Dots with Oxygen-Rich Functional Groups, *J. Am. Chem. Soc.* 134 (2012) 15-18.
- [24] M. Li, W. Wu, W. Ren, H.-M. Cheng, N. Tang, W. Zhong, Y. Du, Synthesis and upconversion luminescence of N-doped graphene quantum dots, *Appl. Phys. Lett.* 101 (2012) 103107.
- [25] C.N.R. Rao, K. Gopalakrishnan, A. Govindaraj, Synthesis, properties and applications of graphene doped with boron, nitrogen and other elements, *Nano Today* 9 (2014) 324-343.
- [26] L.S. Panchakarla, K.S. Subrahmanyam, S.K. Saha, A. Govindaraj, H.R. Krishnamurthy, U.V. Waghmare, C.N.R. Rao, Synthesis, Structure, and Properties of Boron- and Nitrogen-Doped Graphene, *Adv. Mater.* 21 (2009) 4726-4730.
- [27] Y. Shao, Z. Jiang, Q. Zhang, J. Guan, Progress in Nonmetal-Doped Graphene Electrocatalysts for the Oxygen Reduction Reaction, *Chem. Sus. Chem* 12 (2019) 2133-2146.
- [28] S. Zhuang, B.B. Nunna, D. Mandal, E.S. Lee, A review of nitrogen-doped graphene catalysts for proton exchange membrane fuel cells-synthesis, characterization, and improvement, *Nano-Structures & Nano-Objects* 15 (2018) 140-152.
- [29] S.W. Bokhari, A.H. Siddique, H. Pan, Y. Li, M. Imtiaz, Z. Chen, S.M. Zhu, D. Zhang, Nitrogen doping in the carbon matrix for Li-ion hybrid supercapacitors: state of the art, challenges and future prospective, *RSC Adv.* 7 (2017) 18926-18936.
- [30] N.P.D. Ngidi, M.A. Ollengo, V.O. Nyamori, Heteroatom-doped graphene and its application as a counter electrode in dye-sensitized solar cells, *Inter. J. Energy Res.* 43 (2019) 1702-1734.

- [31] M. Han, B.D. Ryu, J.-H. Hyung, N. Han, Y.J. Park, K.B. Ko, K.K. Kang, T.V. Cuong, C.-H. Hong, Enhanced thermal stability of reduced graphene oxide-Silicon Schottky heterojunction solar cells via nitrogen doping, *Mater. Sci. Semicon. Proc.* 59 (2017) 45-49.
- [32] Y. Feng, B. Wang, X. Li, Y. Ye, J. Ma, C. Liu, X. Zhou, X. Xie, Enhancing thermal oxidation and fire resistance of reduced graphene oxide by phosphorus and nitrogen co-doping: Mechanism and kinetic analysis, *Carbon* 146 (2019) 650-659.
- [33] Y. Feng, C. He, Y. Wen, Y. Ye, X. Zhou, X. Xie, Y.-W. Mai, Superior flame retardancy and smoke suppression of epoxy-based composites with phosphorus/nitrogen co-doped graphene, *J. Hazard. Mater.* 346 (2018) 140-151.
- [34] Y. Feng, C. He, Y. Wen, Y. Ye, X. Zhou, X. Xie, Y.-W. Mai, Improving thermal and flame retardant properties of epoxy resin by functionalized graphene containing phosphorous, nitrogen and silicon elements, *Compos. A: Appl. Sci. Manuf.* 103 (2017) 74-83.
- [35] F. Fang, P. Song, S. Ran, Z. Guo, H. Wang, Z. Fang, A facile way to prepare phosphorus-nitrogen-functionalized graphene oxide for enhancing the flame retardancy of epoxy resin, *Compos. Commun.* 10 (2018) 97-102.
- [36] H. Wang, T. Maiyalagan, X. Wang, Review on Recent Progress in Nitrogen-Doped Graphene: Synthesis, Characterization, and Its Potential Applications, *ACS Catal.* 2 (2012) 781-794.
- [37] J.C. Meyer, A.K. Geim, M.I. Katsnelson, K.S. Novoselov, D. Obergfell, S. Roth, C. Girit, A. Zettl, On the roughness of single- and bi-layer graphene membranes, *Solid State Communications* 143 (2007) 101-109.
- [38] F.d. Río, M.G. Boado, A. Rama, F. Guitián, A comparative study on different aqueous-phase graphite exfoliation methods for few-layer graphene production and its application in alumina matrix composites, *Journal of the European Ceramic Society* 37 (2017) 3681-3693.
- [39] S. Sandoval, N. Kumar, A. Sundaresan, C.N.R. Rao, A. Fuertes, G. Tobias, Enhanced Thermal Oxidation Stability of Reduced Graphene Oxide by Nitrogen Doping, *Chem. Eur. J.* 20 (2014) 11999-12003.
- [40] X. Li, H. Wang, J.T. Robinson, H. Sanchez, G. Diankov, H. Dai, Simultaneous Nitrogen Doping and Reduction of Graphene Oxide, *J. Am. Chem. Soc.* 131 (2009) 15939-15944.
- [41] S. Sandoval, N. Kumar, J. Oro-Solé, A. Sundaresan, C.N.R. Rao, A. Fuertes, G. Tobias, Tuning the nature of nitrogen atoms in N-containing reduced graphene oxide, *Carbon* 96 (2016) 594-602.
- [42] D.R. Dreyer, S. Park, C.W. Bielawski, R.S. Ruoff, The chemistry of graphene oxide, *Chem. Soc. Rev.* 39 (2010) 228-240.
- [43] A. Bianco, H.-M. Cheng, T. Enoki, Y. Gogotsi, R.H. Hurt, N. Koratkar, T. Kyotani, M. Monthieux, C.R. Park, J.M.D. Tascon, J. Zhang, All in the graphene family – A recommended nomenclature for two-dimensional carbon materials, *Carbon* 65 (2013) 1-6.
- [44] S. Zhou, A. Bongiorno, Origin of the Chemical and Kinetic Stability of Graphene Oxide, *Sci. Rep.* 3 (2013) 2484.
- [45] D. Wei, Y. Liu, Y. Wang, H. Zhang, L. Huang, G. Yu, Synthesis of N-Doped Graphene by Chemical Vapor Deposition and Its Electrical Properties, *Nano Lett.* 9 (2009) 1752-1758.
- [46] B.C. Brodie, On the Atomic Weight of Graphite, *Philos. Trans. R. Soc. Lond.* 149 (1859) 249-259.
- [47] G.C.C. Costa, O. Shenderova, V. Mochalin, Y. Gogotsi, A. Navrotsky, Thermochemistry of nanodiamond terminated by oxygen containing functional groups, *Carbon* 80 (2014) 544-550.

- [48] G.C.C. Costa, J.K. McDonough, Y. Gogotsi, A. Navrotsky, Thermochemistry of onion-like carbons, *Carbon* 69 (2014) 490-494.
- [49] E.V. Suslova, K.I. Maslakov, S.V. Savilov, A.S. Ivanov, L. Lu, V.V. Lunin, Study of nitrogen-doped carbon nanomaterials by bomb calorimetry, *Carbon* 102 (2016) 506-512.
- [50] J.C. Meyer, A.K. Geim, M.I. Katsnelson, K.S. Novoselov, D. Obergfell, S. Roth, C. Girit, A. Zettl, On the roughness of single- and bi-layer graphene membranes, *Solid State Commun.* 143 (2007) 101-109.
- [51] T.V. Pham, J.-G. Kim, J.Y. Jung, J.H. Kim, H. Cho, T.H. Seo, H. Lee, N.D. Kim, M.J. Kim, High Areal Capacitance of N-Doped Graphene Synthesized by Arc Discharge, *Adv. Funct. Mater.* 1905511, *in press*.
- [52] S. Sandoval, A. Fuertes, G. Tobias, Solvent-free functionalisation of graphene oxide with amide and amine groups at room temperature, *Chem. Commun.* 55 (2019) 12196-12199.
- [53] M. Park, S.-K. Ahn, S. Hwang, S. Park, S. Kim, M. Jeon, Synthesis of Nitrogen-Doped Graphene on Copper Nanowires for Efficient Thermal Conductivity and Stability by Using Conventional Thermal Chemical Vapor Deposition, *Nanomaterials* 9 (2019) 984.